ELSEVIER

Agricultural and Forest Meteorology 81 (1996) 13–29

AGRICULTURAL AND FOREST METEOROLOGY

Carbon dioxide exchange and nocturnal processes over a mixed deciduous forest

Xuhui Lee [a,*], T. Andrew Black [b], Gerry den Hartog [c], Harold H. Neumann [c], Zoran Nesic [b], Janusz Olejnik [d]

[a] *School of Forestry and Environmental Studies, Yale University, New Haven, CT 06511, USA*
[b] *Department of Soil Science, University of British Columbia, Vancouver, B.C., Canada*
[c] *Atmospheric Environment Service, Environment Canada, Downsview, Ont., Canada*
[d] *Department of Agrometeorology, Agricultural University, Poznan, Poland*

Received 20 April 1995; accepted 27 September 1995

Abstract

This paper reports the results of the analysis of CO_2 exchange from a one-month experiment conducted at a mixed deciduous forest, Camp Borden (80°65′ W, 44°19′ N), Canada, in the summer of 1993. The mid-day CO_2 flux from the forest under clear sky conditions was around $-1.0\ mg\,m^{-2}\,s^{-1}$, the average light and water use efficiencies 13 mmol CO_2 (mol photon)$^{-1}$ and 7.95 mg CO_2 (g H_2O)$^{-1}$, and the average nocturnal respiration rate 0.21 mg CO_2 $m^{-2}\,s^{-1}$.

We observed different flow features at heights of 34.5 (14.5 m above the canopy) and 22.4 m at night. Wavelike structures were frequently encountered at $z = 34.5$ m. Depending on the phase angle between the vertical velocity and CO_2 concentration time series, they could act to enhance the co-gradient (upward) flux or to create counter-gradient (downward) flux of CO_2. We speculate that the wave events were limited to isolated regions in the upwind direction. Near the tree-tops ($z = 22.4$ m), the strong wind shear was able to maintain turbulence. Inverse temperature ramp structures were very common and flux of sensible heat was well behaved (directed downward).

1. Introduction

A thorough knowledge of the exchange of CO_2 between forests and the atmosphere is essential in order to better understand forest growth and the role of forest ecosystems in the global atmospheric CO_2 budget. Over the past two decades, many field-scale

* Corresponding author at: School of Forestry and Environmental Studies, Yale University, New Haven, CT 06511, USA. Tel.: +1-203-432-6271; Fax: +1-203-432-3809; E-mail: xhlee@minerva.cis.yale.edu.

SSDI 0168-1923(95)02310-0

investigations have been conducted on the processes of CO_2 exchange between the atmosphere and agricultural crops (Biscoe et al., 1975; McGinn and King, 1990; Rochette et al., 1994; Baldocchi, 1994), a grassland ecosystem (Kim and Verma, 1990), and a windbreak-sheltered orchard (Judd et al., 1993). Recent years have seen a span of experiments carried out in forests, e.g., temperate deciduous forests (Anderson et al., 1986; Verma et al., 1986; Wofsy et al., 1993), a temperate broadleaved evergreen forest (Hollinger et al., 1994), and Douglas-fir forests (Price and Black, 1990; Price and Black, 1991). These researchers have explored to various degrees the possibility of explaining field-scale CO_2 exchange from our understanding of leaf-level biochemistry. Their work has greatly enhanced our knowledge of mechanisms by which environmental factors, such as light, temperature and soil water status, influence the exchange rate.

Although nighttime sensible and latent heat fluxes are small compared to the daytime values, the rate of nighttime respiratory CO_2 release is often of the same magnitude as that of daytime CO_2 uptake by photosynthesis. It is known that a marked difference exists between turbulence regimes within and above forests during the day and at night (Baldocchi and Meyers, 1988; Shaw et al., 1988); however, our knowledge of nocturnal CO_2 exchange is still preliminary. Wofsy et al. (1993) reported that air flow within their forest at night tended to decouple with that above, which caused difficulties in the interpretation of eddy flux of CO_2. Fitzjarrald and Moore (1990) postulated that episodical release of CO_2 due to wave-turbulence events in the canopy can be an important mechanism for the escape of CO_2 built-up within forests to the stratified air above. There is evidence of a correlation between the exchanges of nocturnal CO_2 and sensible heat fluxes (Hollinger et al., 1994). Recognizing the uncertainties in eddy diffusivity at night and the fact that nocturnal CO_2 gradient above the forests often exceeded their instrument capacity, Price and Black (1990, 1991) limited to daytime hours their analysis of data from their Bowen-ratio/energy balance apparatus.

In this paper, we report the results of the analysis of CO_2 exchange from a one-month experiment conducted at a mixed deciduous forest, Camp Borden (80°65′ W, 44°19′ W), Canada, in the summer of 1993. We begin by describing the site and the eddy correlation (EC) systems used in the experiment. Next follows the documentation of the diurnal patterns of the flux over the forest and its light and water use efficiencies. We then focus on nocturnal transport associated with the occurrence of wavelike structures. Time series of two selected runs are examined in detail by spectral methods to gain insights into the process. Finally, in the last section we summarize the conclusions of this analysis.

2. Experimental methods

2.1. Site description

The forest site was well documented by Neumann et al. (1989) and Shaw et al. (1988). Briefly, the forest was about 85 years old and is primarily mixed hardwood with principal species of large-tooth aspen (*Populus grandidentata*) and red maple (*Acer rubrum*). The stand had a height of about 20 m and a LAI of about 5. The fetch is 4 km

over the sector SSE–WNW and 2 km over the sector ENE–SSE. Unless otherwise specified, only data with wind from these sectors are considered for analysis. A 250 m wide red pine plantation lies about 30 m to the N of the measurement tower. The pine was roughly equal in height to the hardwood forest.

2.2. Instrumentation

2.2.1. Eddy correlation and data acquisition

Three EC systems were employed during the field experiment. All EC sensors were mounted 4 m away from a double scaffold tower and pointed to the favorable fetch directions. The first system consisted of a 3-D sonic anemometer/thermometer (Model 1012R2A, Gill Instruments, Lymington, England), a closed-path dual CO_2/H_2O analyzer (Model 6262, LICOR Inc., Lincoln, NE), an open-path H_2O analyzer (Model K20, Campbell Scientific Inc., Logan, UT), and a surface pressure sensor (Model PTA-427, Väisälä, Helsinki, Finland). The signals from the closed-path sensor were amplified by a gain of 10, and together with those from the latter two sensors, were sent to the A/D card in the 3-D unit and two data-loggers. This system was operated at $z = 34.5$ m for most of the experiment and was lowered to $z = 22.4$ m in the later stage for inter-comparison with the second EC system.

Three data acquisition systems were connected in parallel to record the data. A computer was used to receive data (a total of 8 channels) digitized at 20.8 Hz and to carry out on-line data processing. A data-logger (Model 21X, Campbell Scientific Inc.) was used to record the analogue signals at 5 Hz and was also programmed to do on-line computations. Mean statistics generated by this logger were used to fill the gaps when the computer was not in operation. Another data-logger was used to monitor the performance of the closed-path analyzer. Its measurements included CO_2 and H_2O concentrations, gauge pressure and temperature of the air in the sample cell, and optical bench temperature.

The closed-path analyzer was housed in a small box and was regulated at a constant temperature of 45°C. Air was drawn, by a diaphragm pump (Model DOA-V191-AA, GAST Inc., Benton Harbor, MI) at a flow rate of 8.0 l min^{-1}, through a heated sampling tube (Bev-a-line, 3.2 mm id, 3.0 m long) and then a copper tube (3.0 mm id, 1.7 m long) coiled and sandwiched between two aluminum plates, before entering the sample cell. The resulting gauge pressure in the sample cell, monitored with a pressure transducer (Model Motorola MPX 5100, Tempe, AZ), was 22.0 kPa. The closed-path analyzer was operated in absolute mode. A zero gas (ultra pure nitrogen) was passed through the reference cell at a rate of 25 cc min^{-1}.

The open-path analyzer served two purposes. On-line auto-correlation of its signal with the H_2O signal of the closed-path analyzer was formed over the first 5 min of each run to determine the delay time of the latter (Lee et al., 1994). Field tests indicated a very steady delay time of 0.82 s. Water vapour fluxes measured with the two analyzers were compared to evaluate possible tube attenuation.

The open-path analyzer was calibrated against a dew-point generator (Model 610, LICOR Inc.). For the closed-path sensor the factory calibrations were used. Prior to the experiment, its spans were set with gases of known concentrations. Its zero were

checked, and adjusted if necessary, once a day by splitting the reference gas into the sample cell.

The second EC system, mounted at $z = 22.4$ m, was a 3-D sonic anemometer/thermometer (Model SWS-211/3V, Applied Technologies Inc., Boulder, CO). Its signals were digitized at 10 Hz and were sent to the EC computer, where the on-line data processing took place.

The third EC system was operated at $z = 34.5$ m. It consisted of a 3-D sonic anemometer/thermometer (Model DAT-310, Kaijo-Denki Co., Tokyo, Japan), a closed-path CO_2/H_2O analyzer (Model 6262, LICOR Inc.) and analyzers for several other trace gases. Readers are referred to Black et al. (1996) for a detailed description of this system. The three EC systems were later used in the study of the dynamics of carbon dioxide and water vapor fluxes within and above a boreal aspen forest, as part of the BOREAS (Boreal Ecosystem–Atmosphere Study) field campaign. One of the experimental objectives of this study was therefore to identify areas of potential improvement to our systems and to provide a 'baseline calibration' among them so that any bias in the subsequent measurements could be removed.

2.2.2. Supporting measurements

The air temperature profile was measured within and above the stand with thermocouples and aspirated platinum resistance thermometers. A CO_2 profile system was operated during the later stage of the experiment. These measurements indicate that air over the forest was, without exceptions, stably-stratified at night and that CO_2 concentration near the tree-tops was 5–20 ppm higher than that at $z = 35$ m. Other supplementary measurements included wind speed and direction, global, net and photosynthetic active solar radiation densities, relative humidity above the stand, and canopy temperature.

2.3. Data processing

The present analysis relies mainly on the data obtained with the first two EC systems. The averaging time interval was 30 min. All statistics were expressed in the natural coordinate system (Tanner and Thurtell, 1969). Corrections for the density effect were made to CO_2 and H_2O fluxes following Webb et al. (1980).

Nocturnal fluxes were averaged over the period 20:30–6:30 EDT. The rate of storage between the ground and $z = 34.5$ m (height of flux measurements) for this period was estimated from the change in the concentration at $z = 34.5$ m (Hollinger et al., 1994). Analysis of daytime runs was limited to the period 9:00–18:00 EDT, when the rate of change in concentration throughout the stand was very small and for this reason, no storage correction was made to the 30-min flux data.

Spectral analysis was performed for selected runs using the codes of Carter and Ferrie (1979). The phase angle, ϕ, between two time series, x and y, is determined as

$$\phi = \tan^{-1}(Q_{xy}/C_{xy})$$

where Q_{xy} and C_{xy} are the quadrature spectrum and cospectrum, respectively. Here ϕ can be understood as the phase difference between the x and y time series that yields

the greatest correlation for the frequency n (Stull, 1988). The cospectrum is defined such that

$$\overline{x'y'} = \int_0^\infty C_{xy}\,\mathrm{d}n$$

where $\overline{x'y'}$ is the covariance between x and y, and n the natural frequency (Hz).

3. Results and discussion

3.1. Comparison of EC systems

The velocity statistics (mean longitudinal velocity, friction velocity, standard deviations) among the three sonic anemometers agreed to within 8% with the only exception of the longitudinal velocity measured with the second system which was 12% lower. The agreement among the measurements of sensible heat flux was not as satisfactory, with biases ranging from 22% to 17%. After calibrating the sonic units with profile temperature sensors, however, we achieved agreement better than 3%. Good agreement was achieved between the CO_2 fluxes measured with the first and the third systems (slope of regression = 1.05, $R^2 = 0.96$, number of runs = 47).

One major concern with the closed-path EC is the tube attenuation of fluxes. The degree of attenuation depends on three main factors: tube length, tube diameter, and state of air flow within the tube. Air flow was ensured to be turbulent (Reynolds number = 3600), and tube length and diameter were carefully chosen to minimize the attenuation. Using the transfer function recommended by Leuning and King (1992, their Eq. 13) we estimated the upper frequency limit to be about 7 Hz, at which the signal would be reduced by 10% from the full fluctuation. Based on the information on measurement height, wind speed and stability values seen during the experiment, and the spectrum model documented in the classical paper by Kaimal et al. (1972), we estimated that the peak frequency of the vertical velocity-scalar cospectrum should not be higher than 0.05 Hz, which is 2 decades smaller than the upper frequency limit. In other words, we expect no noticeable flux loss owing to tube attenuation. This was further confirmed by the comparison of the latent heat flux measurements with the open- and closed-path analyzers (Fig. 1).

Spectral analysis was performed on the time series for selected periods. There was no discernible difference among the power spectra of temperature, open-path H_2O and closed-path CO_2 across the whole frequency band (0.003–10.4 Hz). The power spectrum of H_2O with the closed-path analyzer, however, displayed a roll-off at about 1 Hz. The roll-off might be caused by the adsorption of water vapor by the sampling tube. Fortunately, it had a negligible effect on the cospectrum with the vertical velocity and for this reason, it did not result in error in the water vapour flux (Fig. 1).

3.2. Daytime and nocturnal CO_2 fluxes

Fig. 2 plots the diurnal variations of CO_2 flux observed on four days. The midday values were around -1 mg m^{-2} s^{-1}, except for August 23, when overcast conditions

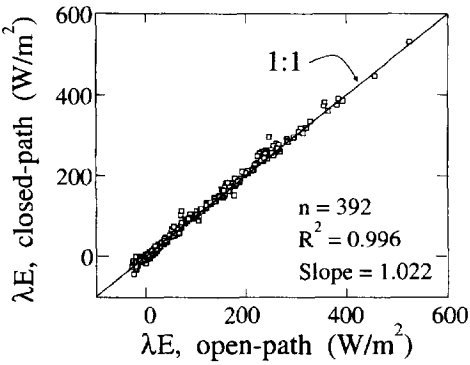

Fig. 1. Comparison of the latent heat flux measured with the closed-path analyzer and that with the open-path analyzer of the first EC system at $z = 34.5$ m.

prevailed. These values were similar to those reported for other fully-leafed deciduous forests (Verma et al., 1986; Wofsy et al., 1993; Hollinger et al., 1994), but, as noted by Verma et al. (1986), they were substantially lower than the peak values measured over agricultural crops (e.g. Baldocchi, 1994; Rochette et al., 1994). The big fluctuations at night were in large part due to the effect of wavelike motions. The daily (24 h) integrated fluxes were (dates in brackets) -13.8 (19), -10.2 (22), -10.0 (23) and -3.6 (24) g m^{-2}.

Fig. 3(a) plots CO_2 flux against the PPFD (photosynthetic photon flux density) and Fig. 3(b) against evapotranspiration rate for the four days. Mean values of the flux and other related variables are listed in Table 1. The average light and water use efficiencies were 0.55 mg CO_2 (mmol photons)$^{-1}$ (13 mmol CO_2 (mol photon)$^{-1}$) and 7.95

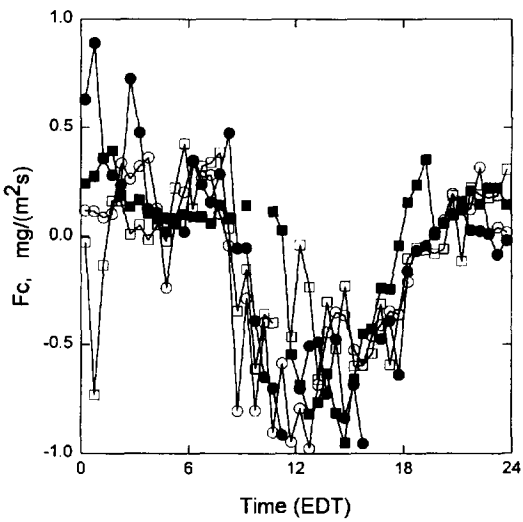

Fig. 2. Diurnal pattern of CO_2 flux at $z = 34.5$ m: ○, 19; ●, 22; □, 23; ■ 24 August.

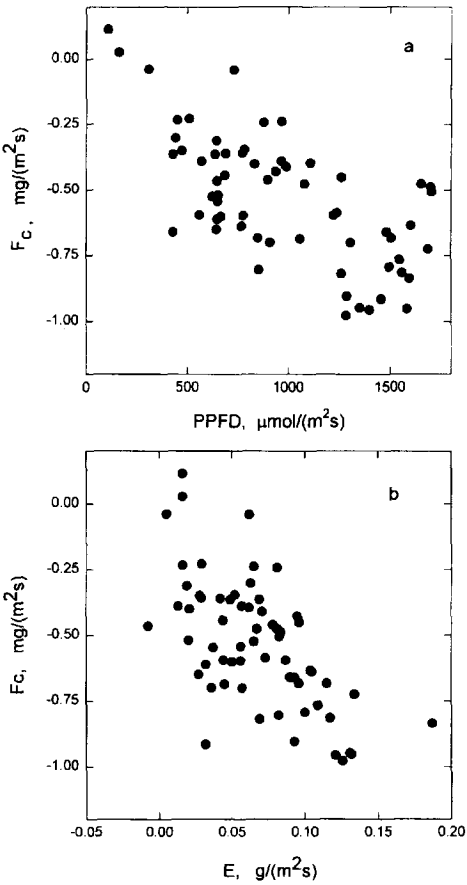

Fig. 3. Plot of daytime (9:30–18:00 EDT) 30-min CO_2 flux against (a) photosynthetic photon flux density ($R^2 = 0.37$, $n = 62$) and (b) evapotranspiration rate ($R^2 = 0.39$, $n = 63$).

mg CO_2 (g water)$^{-1}$. The poor correlation of 30-min CO_2 flux with radiation forcing in Fig. 3(a) seems to be a common pattern for forest stands (e.g., Verma et al., 1986; Hollinger et al., 1994). On the other hand, the daytime CO_2 flux over agricultural crops

Table 1
Daytime (9:30–18:00 EDT) averages of photosynthetic photon flux density (PPFD), canopy temperature (T_c), saturation vapor pressure deficit (D), fluxes of latent heat (λE), sensible heat (H) and CO_2 (F_c) and CO_2 rate of storage (S_c) at the deciduous forest, Camp Borden, Canada, in August 1993

Date	PPFD (μmol m^{-2} s^{-1})	T_c (°C)	D (hPa)	λE (W m^{-2})	H (W m^{-2})	F_c (mg m^{-2} s^{-1})	S_c (mg m^{-2} s^{-1})	$F_c + S_c$ (mg m^{-2} s^{-1})
19	968	30.5	14.2	186	29	−0.584	−0.041	−0.624
22	1264	25.5	11.1	217	139	−0.649	−0.060	−0.709
23	601	23.0	7.0	85	−10	−0.426	−0.079	−0.505
24	955	29.4	8.3	116	83	−0.470	−0.034	−0.504

Table 2
Same as in Table 1 except for nighttime (20:30–6:30 EDT) averages, where u_* is the friction velocity at $z = 34.5$ m

Date	T_c (°C)	u_* ($m s^{-1}$)	F_c ($mg m^{-2} s^{-1}$)	S_c ($mg m^{-2} s^{-1}$)	$F_c + S_c$ ($mg m^{-2} s^{-1}$)
18–19	22.5	0.15	0.113	0.121	0.234
19–20	24.9	0.13	0.077	0.067	0.143
21–22	12.6	0.11	0.244	0.117	0.361
22–23	16.3	0.11	0.023	0.119	0.142
23–24	23.7	0.43	0.170	0.001	0.171
24–25	24.6	0.31	0.159	0.054	0.213

generally correlates well with PPFD (Rochette et al., 1994; Baldocchi, 1994). Instead of using 30-min observations, Wofsy et al. (1993) averaged their flux over morning and afternoon hours and obtained the flux-light response curves with a clearly-defined light compensation point and the tendency to saturate at the high light level. Our sample size is, however, too small for us to try their approach. The poor correlation may suggest that the ecophysiology of CO_2 exchange at the forest stand level has a time scale much longer than the 30-min interval commonly used in eddy correlation calculations.

Table 2 lists the nighttime observations over the forest. The storage term was a significant component of the nocturnal CO_2 exchange when the friction velocity was small, i.e., when the ventilation was poor. The nocturnal respiration rate of this forest stand ($F_c + S_c$), averaged over the 6 nights, was 0.21 $mg m^{-2} s^{-1}$, similar to the summer values observed at other forests (Hollinger et al., 1994; Wofsy et al., 1993; Price and Black, 1990).

While statistical analysis of the relation between the respiration rate and temperature is not feasible because of the small number of samples, the very high value observed during the night August 21–22 deserves some attention. A frontal system passed the site on the night of August 20, causing a large decrease in foliage temperature. The foliage temperature during the night August 21–22 was 12.3 °C lower than that during the night August 19–20 and yet the respiration rate was rather high, and in fact, the highest among all nights. This unusual feature might suggest that the foliage respiration rate be small compared to that of the soil respiration, a process largely controlled by soil temperature which should have been rather insensitive to the frontal disturbance. With a much larger number of nighttime observations, the exercise of multi-variate regression of the respiration rate against soil and foliage temperatures should allow us to quantitatively discern the soil and foliage contributions to the observed net ecosystem exchange. Because wave events occurred frequently at night, there is also the possibility that the correlation of nocturnal respiration to environmental temperature was obscured by the effect of wavelike motions.

3.3. Transport by wavelike structures

3.3.1. General features

Fig. 4 plots the time series of a 3-hour period. Profile measurements indicate that the inversion layer extended from mid-canopy to the top of the tower (height 45 m)

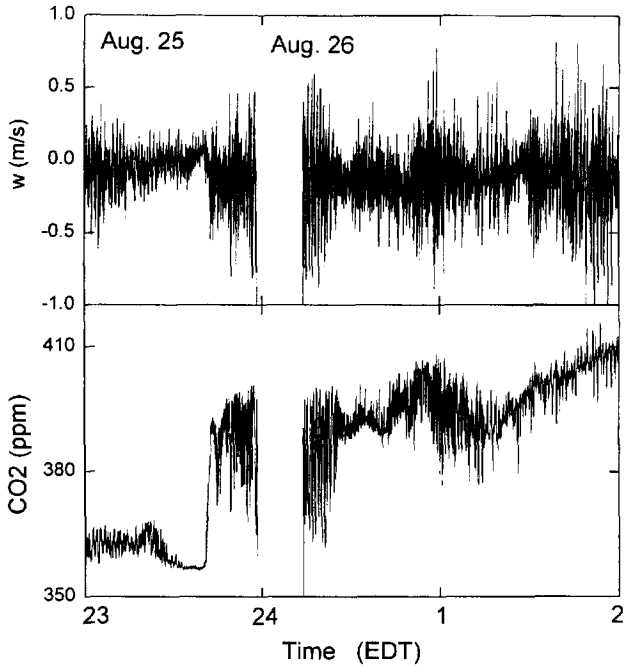

Fig. 4. Time series of the vertical velocity and CO_2 concentration at $z = 34.5$ m during the night August 25–26.

throughout the night of August 25–26. On the evening of August 25, the wind was from the North, where there was a 250-m strip of pine plantation between the tower and agricultural land. A sudden wind direction change occurred around midnight. After that, the wind was from WSW, a sector with an extensive deciduous forest coverage. Associated with the direction shift was a 40 ppm increase in CO_2 concentration, a 3°C decrease in air temperature, a 2.6 $g\,m^{-3}$ increase in water vapor density and a 10 ppb decrease in O_3 concentration. Interestingly, no noticeable step changes occurred at $z = 22.4$ m. Assuming that the pine plantation was similar to the deciduous forest in its surface characters, the dramatic changes at $z = 34.5$ m suggest that the footprint at this height must have been much bigger than 250 m.

The large fluctuations in both w and CO_2 concentration in Fig. 4 were a result of wavelike motions, which are best shown in Fig. 5. These wavelike features frequently appeared in the time series during the experiment. They usually lasted about 10–15 min and were followed by an interval without clear periodic patterns. Large fluctuations in CO_2 concentration were recorded during these wavelike events. In fact, the 30-min standard deviation can be used as a diagnostic indicator of its occurrence. For the experiment reported here, the threshold value was about 10 ppm, above which wavelike oscillations can be seen in the time series.

The wavelike episodes tended to occur when there was a very weak wind shear and a strong inversion (net radiation flux $< -60\ W\,m^{-2}$). At the lower height ($z = 22.4$ m) a

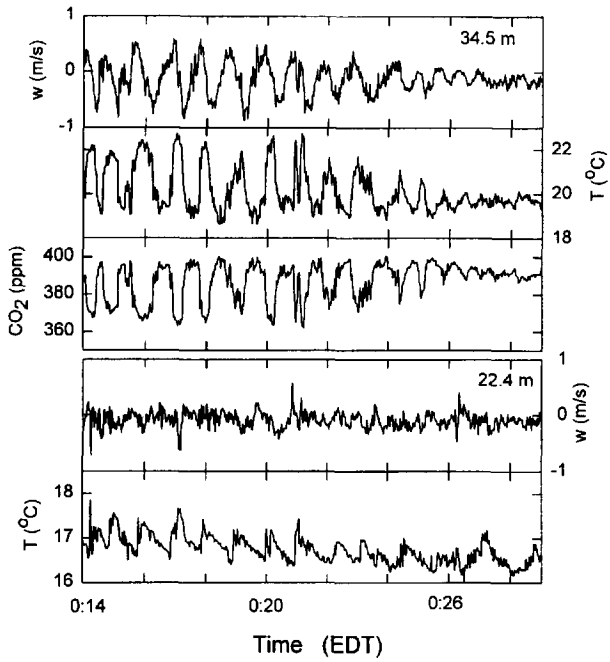

Fig. 5. Time series showing wavelike oscillations at $z = 34.5$ m and inverse temperature ramps at $z = 22.4$ m on August 26.

much stronger wind speed gradient existed, so not surprisingly, inverse temperature ramps were very common (Fig. 5). It is interesting to note that there is an obvious phase relationship between the ramps at $z = 22.4$ m and the wavelike motions at $z = 34.5$ m. Paw U et al. (1992, 1990, 1989) also witnessed the synchronous occurrence of ramps and waves in an almond orchard canopy, which they believed may imply close linkage between the two forms of motions.

3.3.2. Counter-gradient flux

Fitzjarrald and Moore (1990) reported that wavelike episodes within and near the top of an Amazonian forest accounted for significant release of CO_2 from the forest at night. In the present study, waves acted on some occasions to enhance co-gradient fluxes of CO_2 and sensible heat at $z = 34.5$ m, while on other occasions to create counter-gradient fluxes (downward CO_2 flux and upward sensible heat flux). These abnormal fluxes were observed during 18% of the nocturnal runs. The wavelike events were responsible for the nighttime 'spikes' that appear in the diurnal plots of CO_2 flux (Fig. 2). Near the tree-tops ($z = 22.4$ m), however, sensible heat flux (the only scalar flux observed at this height) was much better behaved: it was directed downward (co-gradient flux) for $> 99\%$ of the nighttime runs. For practical purposes, it may therefore be advantageous to position the observation system near the top of the stand.

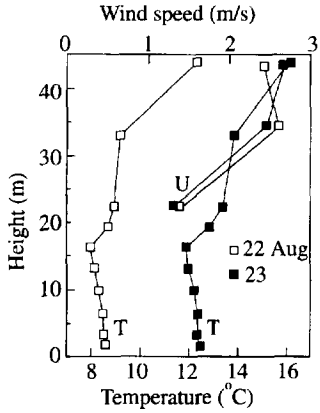

Fig. 6. Vertical profiles of wind speed (U), air temperature (T) for the period 0:30–1:00 EDT August 22 (Run 22002) and 0:30–1:00 EDT August 23 (Run 23002).

3.3.3. *Spectral representation of time series*

To gain insights into the mechanism by which wavelike events transport CO_2, we selected two typical runs for detailed analysis. No CO_2 profile data were available during these periods, but it is safe to assume a negative vertical gradient over the forest (higher concentration near the tree-tops than above). The profiles of mean air temperature and wind speed are plotted in Fig. 6 and mean statistics are listed in Table 3. Run 22002 shows enhanced co-gradient sensible heat and CO_2 fluxes at $z = 34.5$ m due to waves, while Run 23002 is an example of counter-gradient fluxes. The magnitude of CO_2 flux is as big as that observed at mid-day under full sunshine.

Fig. 7 shows the cospectrum between the vertical velocity and CO_2 concentration for the two runs. A prominent peak occurred around 0.016 Hz for both runs, consistent with the wave period of about 65 s determined from an autocorrelation procedure. The wave period reported here is larger than that observed by Paw U et al. (1989) (44 s) in a almond orchard and is lower than that observed by Fitzjarrald and Moore (1990) (65–80 s) near the top of their forest. In a study of a very stable atmospheric boundary layer, Smedman (1988) reported wavelike motions with very long period (208 min) at a height

Table 3
Mean statistics for the two runs indicated in Fig. 6: CO_2 flux (F_c), sensible heat flux (H), momentum flux ($\overline{u'w'}$)

Run	Height (m)	F_c (mg m^{-2} s^{-1})	H (W m^{-2})	$\overline{u'w'}$ (m^2 s^{-2})
22002	34.5	0.89	−99	−0.000
	22.4		−16	−0.030
23002	34.5	−0.73	53	0.009
	22.4		−19	−0.022

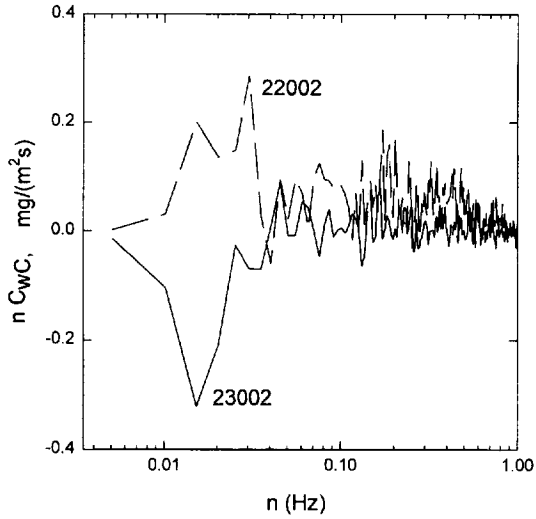

Fig. 7. Cospectrum between the vertical velocity component and CO_2 concentration at $z = 34.5$ m for Runs 22002 and 23002.

of 30 m, although the author did not rule out the possibility that there was a trend in the time series. In another related study, Maitani (1989) observed wavelike fluctuations of temperature and wind velocity with a period of 15–29 min and approximately equal contributions to sensible heat flux from wavelike and turbulent motions. Unlike his study, our cospectrum in the high frequency range, where turbulent eddies made their contribution, was more scattered and less significant in comparison with that at the wave frequency.

To separate wave and turbulence contributions, Finnigan et al. (1984) proposed a triple decomposition procedure. The implementation of this procedure requires a reference oscillator, which is not available in the present study. Instead, we resorted to a moving average scheme to further quantify the role of the waves. CO_2 flux was calculated as

$$F_c(\tau) = \frac{1}{T}\int_0^T \left[w(t) - \overline{w}(t,\tau)\right]\left[C(t) - \overline{C}(t,\tau)\right] \mathrm{d}t$$

where

$$\overline{w}(t,\tau) = \frac{1}{\tau}\int_{t-\tau/2}^{t+\tau/2} w(x)\,\mathrm{d}x$$

and

$$\overline{C}(t,\tau) = \frac{1}{\tau}\int_{t-\tau/2}^{t+\tau/2} C(x)\,\mathrm{d}x$$

are moving averages of the vertical velocity and CO_2 concentration over interval τ, and $T = 30$ min. Here $F_c(\tau)$ can be understood as the total contribution to the flux from motion with periods $< \tau$. When τ is sufficiently small, the part due to low-frequency

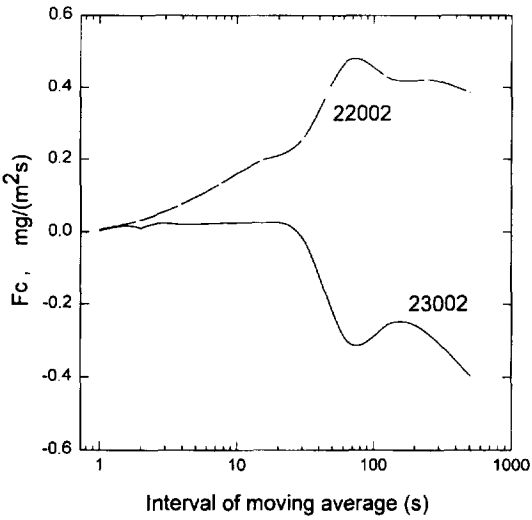

Fig. 8. CO_2 flux calculated using different moving intervals (Runs 22002 and 23002).

waves will be filtered out, leaving only the turbulence contribution. The results are plotted in Fig. 8. In the lower range of τ, the calculated flux is positive for both runs, indicating that the turbulence contribution is essentially down the mean concentration gradient. As τ increases from about half of the wave period, $F_c(\tau)$ increases (decreases) rapidly for Run 22002 (23002). But $F_c(\tau)$ levels off beyond the wave period. Taking 16 s as the threshold at which $F_c(\tau)$ for Run 23002 is largest or in other words, the wave contribution is not yet in effect, we can use the information in Fig. 8 to arrive at a rough estimate of the relative importance of wave and turbulent motions in the transport of CO_2. The ratio of the turbulence contribution to the wave counterpart was 0.7 for Run 22002 and -0.1 for Run 23002. These values were in rough accord with the ratios obtained by integrating the cospectral energy over high ($n > 0.06$ Hz) and low ($n < 0.06$ Hz) frequency ranges. The overriding role of waves in Run 23002 is a consequence of the fact that the phase angle between the time series of the vertical velocity and CO_2 concentration deviates significantly from 90° (see below).

From the temperature profiles in Fig. 6, we can calculate the Brunt–Väisälä frequency as

$$N = \left[\left(\frac{g}{\theta}\right)\frac{\partial\theta}{\partial z}\right]^{0.5}$$

where g is the gravitational acceleration and θ the potential temperature. Here N is the frequency of gravity waves in a stable atmosphere (Tennekes and Lumley, 1972). But in a situation where the temperature gradient varies with height, N is not necessarily the frequency of a trapped gravity wave (Paw U et al., 1989). For Run 22002, N equals 0.085 Hz in the air layer 35–45 m and 0.042 Hz in the layer 22–35 m. The corresponding values for Run 23002 were 0.100 and 0.034 Hz. These values were much higher than the observed wave frequency of 0.016 Hz, so it is safe to argue that the

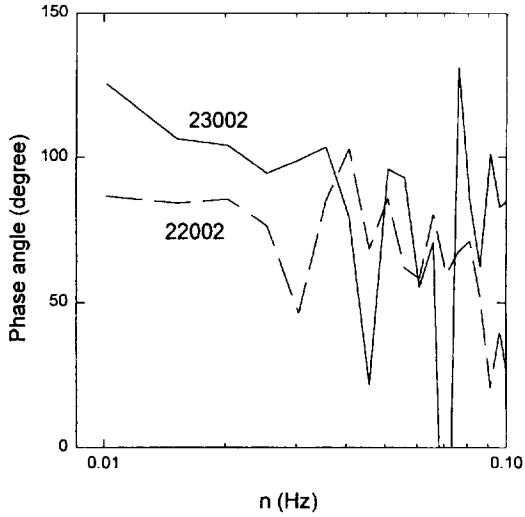

Fig. 9. Same as in Fig. 7 except for phase angle.

waves encountered here are not pure gravity waves. This is further demonstrated by the phase angle distribution (Fig. 9). For gravity waves, a phase angle of 90° between the vertical velocity and CO_2 concentration is expected, in which case they would not contribute to the flux. Fig. 9 indicates a phase angle of about 80° for Run 22002 and 100–120° for Run 23002 over the frequency range 0.005–0.03 Hz. So in the phase domain, whether waves act to enhance co-gradient flux or to create counter-gradient flux depends on the phase angle: co-gradient flux if less than 90° and counter-gradient flux if greater than 90°. This naturally leads to the question of whether the phase angle can be linked to the background forcing variables that could be easily measured, and therefore be useful as a diagnostic tool for predicting the occurrence of the counter-gradient flux. To seek the answer, we separated runs with wave structures into two categories, one with co-gradient fluxes and the other with counter-gradient fluxes. There does not appear to be an appreciable difference between the two in the external parameters such as Richardson number, temperature gradient, gradient of wind speed and net radiation flux.

A review of the literature suggests that the prediction of the phase angle from the background forcing cannot be easily achieved. A good illustration of this is the work of Finnigan et al. (1984). Their calculations of, for example, phase velocity and period, from a linear stability analysis were in good agreement with the measurements, but their calculations of the phase difference between the vertical velocity and temperature time series were very poor in terms of agreement with observations. In another related study, Fitzjarrald and Moore (1990) proposed a resonance wave model which captured some important features observed during their experiment. Their modelled time series, however, are not presented with a time resolution fine enough to allow an examination of the phase difference.

4. Conclusions

From our observations we found that the mid-day CO_2 flux under clear sky conditions was about $-1.0\ mg\,m^{-2}\,s^{-1}$, the average light and water use efficiencies 13 mmol $CO_2\,(mol\,photon)^{-1}$ and 7.95 $mg\,CO_2\,(g\,H_2O)^{-1}$, and the average nocturnal respiration rate 0.21 $mg\,CO_2\,m^{-2}\,s^{-1}$. The correlation between 30-min CO_2 flux and PPFD was, however, rather poor.

We have observed different flow features at $z = 34.5$ and 22.4 m at night. Wavelike structures were frequently encountered at $z = 34.5$ m. Depending on the phase angle between the vertical velocity and CO_2 concentration time series, they could act to enhance the co-gradient (upward) flux or to create a counter-gradient (downward) flux of CO_2. These structures were associated with very large fluctuations in CO_2 concentration, and in the present study the threshold value of 30-min standard deviation was 10 ppm, above which wavelike events can be seen in the time series.

Near the tree-tops ($z = 22.4$ m), the strong wind shear was able to maintain turbulence. Inverse temperature ramp structures were very common and the flux of sensible heat was well behaved (directed downward).

Mahrt (1988) has listed five serious problems related to the estimation of fluxes and other statistical quantities in strongly stratified flow, and in particular, in the presence of waves. Added to the list is the question of spatial patchiness. If a large counter-gradient CO_2 flux occurred uniformly in space in the upwind direction, one would expect a rapid build-up in CO_2 concentration in the air layer below the observation level. For example, for a downward flux of $0.73\ mg\,m^{-2}\,s^{-1}$ at $z = 34.5$ m (Run 23002), the expected increase in the average CO_2 concentration in the 34.5 m air layer would reach 40 $mg\,m^{-3}$ over a 30-min interval. If the respiration contribution from the forest was included in the calculation, then the increase would be even faster. There is no evidence of build-up of this magnitude during this experiment and the experiment we carried out later in a boreal aspen forest. One likely scenario is that waves occur in patches. They can 'pump' CO_2 into isolated pockets of air which are then transported away from the local region by the mean wind. When such a scenario happens, fluxes at the height of wave occurrence should be interpreted as apparent fluxes, which obviously will not reflect the ecophysiology of the forest. Because of the difficulty in interpreting observations when waves are present, it may therefore be advantageous to lower the eddy correlation system to a level near the top of the stand where a stronger wind shear is expected and waves are less likely to occur.

Acknowledgements

The authors appreciate the assistance with the experiment by Dr. Jose Fuentes, Dr. Grant Edward, Peter Blanken, John Deary, Isobel Simpson, Ralph Staebler, and Paul Yang. Comments by Dr. K.T. Paw U and the two reviewers are gratefully acknowledged.

References

Anderson, D.E., Verma, S.B. and Clement, R.J., 1986. Turbulence spectra of CO_2, water vapor, temperature and velocity over a deciduous forest. Agric. For. Meteorol., 38: 81–99.

Baldocchi, D.D., 1994. A comparison study of mass and energy exchange over a closed (wheat) and an open (corn) canopy. II: CO_2 exchange and water use efficiency. Agric. For. Meteorol., 67: 291–321.

Baldocchi, D.D. and Meyers, T.P., 1988. Turbulence structure in a deciduous forest. Boundary-Layer Meteorol., 43: 345–364.

Biscoe, P.V., Scott, R.K. and Monteith, J.L., 1975. Barley and its environment. III: Carbon budget of the stand. J. Appl. Ecol., 12: 269–293.

Black, T.A., den Hartog, G., Neumann, H.H., Blanken, P.D., Yang, P.C., Russell, C., Nesic, Z., Lee, X., Chen, S.G. and Staebler, R., 1996. Annual cycles of water vapor and carbon dioxide fluxes in and above a boreal aspen forest. Global Change Biol., in press.

Carter, G.C. and Ferrie, J.F., 1979. A coherence and cross spectral estimation program. In: Digital Processing Committee (Editors), Programs for Digital Signal Processing. IEEE Press, Chap. 2.3.1–2.3.18.

Finnigan, J.J., Einaudi, F. and Fua, D., 1984. The interaction between an internal gravity wave and turbulence in the stably-stratified nocturnal boundary layer. J. Atom. Sci., 41: 2409–2436.

Fitzjarrald, D.R. and Moore, K.E., 1990. Mechanims of nocturnal exchange between the rain forest and the atmosphere. J. Geophys. Res., 95D: 16839–16850.

Hollinger, D.Y., Kelliher, F.M., Byers, J.N., Hunt, J.E., McSeveny, T.M. and Weir, P.L., 1994. Carbon dioxide exchange between an undisturbed old-growth temperate forest and the atmosphere. Ecology, 75: 134–150.

Judd, M.J., Prendergast, P.T. and McAneney, K.J., 1993. Carbon dioxide and latent heat flux measurements in a windbreak-sheltered orchard. Agric. For. Meteorol., 66: 193–210.

Kaimal, J.C., Wyngaard, J.C., Izumi, Y. and Cote, O.R., 1972. Spectral characteristics of surface layer turbulence. Q. J. R. Meteorol. Soc., 98: 563–589.

Kim, J. and Verma, S.B., 1990. Carbon dioxide exchange in a temperature grassland ecosystem. Boundary-Layer Meteorol., 52: 135–149.

Lee, X., Black, T.A. and Novak, M.D., 1994. Comparison of flux measurements with open- and closed-path gas analyzers above an agricultural field and a forest floor. Boundary-Layer Meteorol., 67: 195–202.

Leuning, R. and King, K.M., 1992. Comparison of eddy-covariance measurements of CO_2 fluxes by open- and closed-path CO_2 analyzers. Boundary-Layer Meteorol., 59: 297–311.

Mahrt, L., 1988. Turbulence in stratified flow. 8th AMS Symposium on Turbulence and Diffusion, pp. 131–135 (preprint).

Maitani, T., 1989. Wave-like wind fluctuations observed in the stable surface layer over a plant canopy. Boundary-Layer Meteorol., 48: 19–31.

McGinn, S.M. and King, K.M., 1990. Simultaneous measurements of heat water vapour and CO_2 fluxes above alfalfa and maize. Agric. For. Meteorol., 49: 331–349.

Neumann, H.H., den Hartog, G. and Shaw, H.H., 1989. Leaf area measurements based on hemispheric photographs and leaf-litter collection in a deciduous forest during autumn leaf-fall. Agric. For. Meteorol., 45: 325–345.

Paw U, K.T., Brunet, Y., Collineau, S., Shaw, R.H., Maitani, T., Qiu, J. and Hipps, L., 1992. On coherent structures in turbulence above and within agricultural plant canopies. Agric. For. Meteorol., 61: 55–68.

Paw U, K.T., Shaw, R.H. and Maitani, T., 1990. Gravity waves in an almond orchard. 9th AMS Symposium on Turbulence and Diffusion, pp. 244–246 (preprint).

Paw U, K.T., Shaw, R.H., Maitani, T. and Cionco, R.M., 1989. Gravity waves in an almond orchard. 19th AMS Conference on Agricultural and Forest Meteorology, pp. 184–185 (preprint).

Price, D.T. and Black, T.A., 1991. Effects of summertime changes in weather and root-zone soil water storage on canopy CO_2 flux and evapotranspiration of two juvenile Douglas-fir stands. Agric. For. Meteorol., 53: 303–323.

Price, D.T. and Black, T.A., 1990. Effects of short-term variation in weather on diurnal canopy CO_2 flux and evapotranspiration of a juvenile Douglas-fir stand. Agric. For. Meteorol., 50: 139–158.

Rochette, P., Desjardins, R.L., Patty, E. and Lessard, R., 1994. Measurement of crop net carbon dioxide

exchange rate in soybean. 21st AFM Conference on Agricultural and Forest Meteorology, pp. 259–260 (preprint).

Shaw, R.H., den Hartog, G. and Neumann, H.H., 1988. Influence of foliar density and thermal stability on profiles of Reynolds stress and turbulence intensity in a deciduous forest. Boundary-Layer Meteorol., 45: 391–409.

Smedman, A., 1988. Observations of a multi-level turbulence structure in a very stable atmospheric boundary layer. Boundary-Layer Meteorol., 44: 231–253.

Stull, R.B., 1988. An Introduction to Boundary Layer Meteorology. Kluwer, Boston, MA.

Tanner, C.B. and Thurtell, G.W., 1969. Anemoclinometer measurements of Reynolds stress and heat transport in the atmospheric surface layer. Research and Development Technical Report ECOM-66-G22F, University of Wisconsin, Madison, WI.

Tennekes, H. and Lumley, J.L., 1972. A First Course in Turbulence. MIT Press, Cambridge, MA.

Verma, S.B., Baldocchi, D.D., Anderson, D.E., Matt, D.R. and Clement, R.J., 1986. Eddy fluxes of CO_2, water vapor, and sensible heat over a deciduous forest. Boundary-Layer Meteorol., 36: 71–91.

Webb, E.K., Pearman, G.I. and Leuning, R., 1980. Correction of flux measurements for density effects due to heat and water vapour transfer. Q. J. R. Meteorol. Soc., 106: 85–100.

Wofsy, S.C., Goulden, M.L., Munger, W., Fan, S.-M., Bakwin, P.S., Daube, B.C., Bassow, S.L. and Bazzaz, F.A., 1993. Net exchange of CO_2 in a mid-latitude forest. Science, 260: 1314–1317.